J. Fluid Mech. (1996), vol. 325, pp. 377–397

The effect of entrained air in violent water wave impacts

By D. H. PEREGRINE AND L. THAIS
School of Mathematics, University of Bristol, Bristol BS8 1TW, UK

(Received 29 February 1996 and in revised form 25 May 1996)

The effects of entrained air in cushioning water impact on a wall are estimated by using a flow which has many similarities to the severe flip-through impacts that have been identified for water waves hitting a vertical wall. This is a filling flow which rapidly fills a confined region, such as a crack between blocks, or the space beneath a deck projecting from the coast (Peregrine & Kalliadasis 1996). The main properties of the filling flow are easily calculated, including the high-pressure peak which corresponds to the pressure peak of a flip-through. This work extends the study of filling flows to the case where the filling liquid is an air–water mixture, thus giving explicit results for the reduction of peak pressure due to the compressibility of entrained air. The behaviour of a bubbly liquid subject to substantial pressure changes is considered. Expressions are derived for an air–water mixture treated as a compressible fluid. The reduction in pressure from the incompressible case is found to be large even for relatively small air content, and depends more on the reduction in fluid volume than any other feature of the pressure–density relation. Results are presented in such a way that they may be used to estimate compressibility corrections to both the maximum and background pressures in a flip-through wave impact if corresponding incompressible pressure values are available.

1. Introduction

In the study of the impact of water waves there has long been a problem in scaling experimental data from laboratory to prototype scales. The natural choice is Froude scaling, since the incident waves are surface gravity waves: however, this choice gives unrealistically large prototype forces. The severity of the pressures and short time scales of the motion lead to the view that compressibility becomes important within large ocean waves. This view is strengthened by the fact that in most practical cases of severe impact there is substantial mixing of air and water, and once water has entrained air, even small volume fractions give greatly increased compressibility. Experimental evidence includes pressure oscillations recorded on sea walls or in the laboratory, where the compressibility of the fluid is mainly attributed to the presence of air in the water (e.g. Hattori & Arami 1992; Schmidt, Oumeraci & Partenscky 1992).

There are two obvious ways in which air cushions wave impact. One is when a pocket of air is trapped and effectively spreads the impact pressure in both space and time. The trapping of air in this manner and the resulting effect on the pressures, especially the way in which they oscillate due to volume changes of the trapped air pocket is the topic of the theoretical studies by Bagnold (1939), Ramkema (1978), Peregrine (1994), Topliss, Cooker & Peregrine (1992), Topliss (1994), Peregrine &

Topliss (1994), and Zhang, Yue & Tanizawa (1996). If no air is trapped very high pressures are generated in the flip-through motion identified by Cooker & Peregrine (1990*a*,*b*, 1992, 1996). In flip-through the wave actually does not hit the wall but shoots up without trapping any air bubble. Then the second way in which air might cushion an impact becomes important. That is by its entrainment and suspension as small bubbles in the water. This is especially relevant to coastal situations since the general size of bubbles in salt water is very much smaller than in fresh water and in an environment where waves are frequently breaking the volume fraction of air is likely to be over 1%. Since the most violent impacts appear to be due to flip-through, or when a trapped air pocket is particularly small, it is desirable to assess how compressibility of the fluid affects flip-through.

Once compressibility of the fluid is taken into account simplifications that allow computation with Laplace's equation are no longer applicable. However, Peregrine & Kalliadasis (1996, referred to as PK hereafter) have discovered a flow which has many similarities to the flow in a flip-through wave impact at the time of maximum pressure. This is a flow rapidly filling a confined region, such as a crack between blocks, or the space beneath a deck projecting from the coast. The main properties of the filling flow are easily calculated, including the high-pressure peak which corresponds to the pressure peak of a flip-through. This work extends the study of filling flows to the case where the filling liquid is an air–water mixture, thus giving explicit results for the reduction of peak pressure due to the compressibility of entrained air. Most previous studies on the compressibility of bubbly liquids on wave impact have only considered the acoustic regime where small pressure departures from equilibrium are allowed. Here the behaviour of a bubbly liquid subject to substantial pressure changes is considered.

In §2 we give a brief review of the incompressible filling flow of PK. In §3 we analyse the compressible version of the same flow. The compressibility effects are modelled by assuming that incompressible water contains an incoming volume fraction, β_1, of air dispersed in homogeneously distributed small bubbles. The equation of state for the bubbly mixture is discussed and the integral in Bernoulli's equation evaluated. The results, presented in §4, show how the air significantly reduces the pressures in the flow. The pressure reductions depend on the inflow Mach number and the severity of the corresponding incompressible flow. An approximate solution is derived that gives the quantities of importance in the flow, namely the background and maximum pressures, in a surprisingly simple manner. The approximation also shows that the major cause of the cushioning of high pressures by the dispersed air is the volume reduction at high pressures. This reduces the speed of filling, which in turn leads to lower pressures. The analogy with flip-through that stimulated discovery of the filling flow is used to provide guidance for compressibility corrections to incompressible estimates of pressures imposed by water wave impacts. The corrections for maximum pressures differ from those for the background pressure found below the point of peak pressure on a wall. The discussion in §5 gives an example of a comparison with flip-through pressures, and guidance on how to use the results of the previous section. Section 6 gives a brief discussion of the supersonic flow and shock wave that could result from wave impact.

2. Incompressible filling flow

The filling flow defined by PK describes an incoming flow of height h, velocity V_1 horizontally entering and rapidly filling a container of height H. The container is

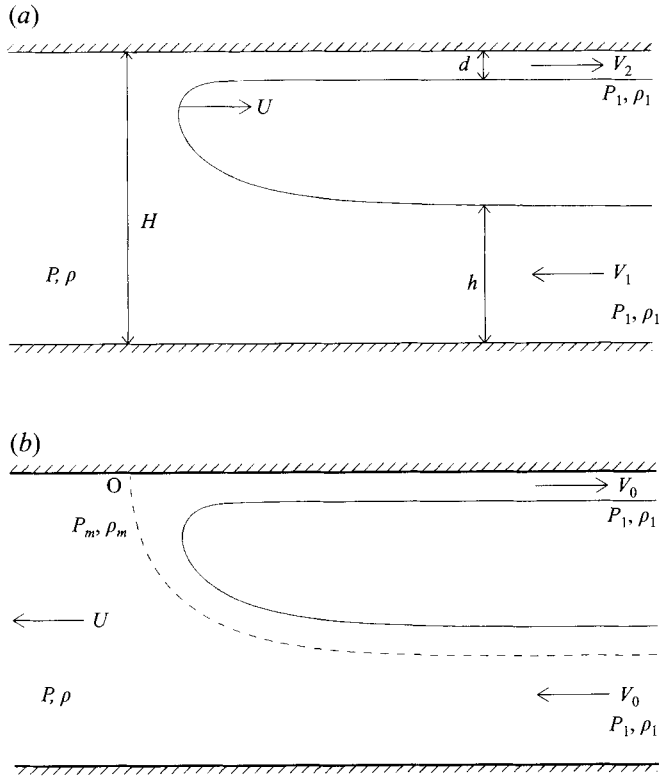

FIGURE 1. Configuration of the filling flow: (*a*) in the stationary frame of reference, (*b*) in the moving frame of reference (free-surface profiles are plotted for examples of the incompressible flow, $k = 0.684, \epsilon = 0.532$, see PK).

being filled with a velocity U, and there is a thin backflow at the top with velocity V_2 and thickness d, see figure 1(*a*). This flow may occur where a water wave enters beneath a horizontal coastal structure or into a crack in a cliff and henceforth rapidly fills up the available space. The case where h/H is almost 1 and hence U is large is of special interest because of the high pressures generated. This flow is related to flip-through by an observation of Cooker that at the time of peak pressure in a flip-through the flow is forming a jet and the pressure peak moves with almost constant velocity giving a quasi-steady behaviour (Cooker & Peregrine 1996). Accordingly, the filling flow is considered to be steady in the reference frame moving with velocity U from left to right; the velocity at the far end of the already-filled portion of the container is then no longer zero but U from right to left, see figure 1(*b*). Thus the flow divides and the pressure is maximum at the stagnation point, O, in the moving reference frame.

PK show that little algebra is required to solve for the global properties of the incompressible flow. This is achieved by writing two kinematic conditions, a mass-conservation equation, a momentum-flux equation and Bernoulli's equation, see equations (1) to (4) in PK. With the further assumption that gravity may be neglected in the especially violent motions PK gives the following expressions for the maximum pressure $p_m^{(i)}$, the background, or filling, pressure in the portion of the space already filled, $p^{(i)}$, and the width of the small outward-flowing jet, $x^{(i)} = d/H$, where the

superscript (i) stands for incompressible solution:

$$p^{(i)} = \frac{k}{1-k}, \tag{2.1a}$$

$$p_m^{(i)} = \frac{1}{4(1-k)^2}, \tag{2.1b}$$

$$x^{(i)} = (1-k)^2, \tag{2.1c}$$

where $k = (h/H)^{1/2}$ is the square root of the fraction of the cross-section of the container being filled by the incoming jet. The pressures are normalized with $\frac{1}{2}\rho_l V_1^2$, where ρ_l denotes density of water. When k is close to 1 both pressures $p^{(i)}$ and $p_m^{(i)}$ become large. For example when the inward jet occupies 81% of the container height, H, it induces a background pressure of 9 and a maximum pressure of 25 at the point O, whereas the outward jet thickness is only 1% of the container height.

3. Filling flow with entrained air

3.1. *Basic assumptions*

We now turn to the generalization of the conservation equations for the case of a compressible air–water mixture. We keep the assumption that the pressure is constant along the free streamline. Since gravity is neglected for the violent flows we are interested in, the velocity is a constant V_0 along the free steamline in the moving reference frame, just as for the incompressible flow. PK have shown that this assumption is appropriate for Froude numbers $\mathscr{F}_r = V_1/(gH)^{1/2}$ of order or larger than 1, and we expect this to hold for the compressible flow. Thus, the kinematic relations of relative velocity

$$V_0 = V_1 + U, \tag{3.1a}$$

$$V_0 = V_2 - U \tag{3.1b}$$

hold at the two extremes of the free streamline.

At this stage it is necessary to make assumptions concerning the behaviour of the bubbly liquid. Most studies of compressibility of gas–liquid mixtures have been concerned with the propagation of small-amplitude disturbances. Sangani (1993) gives a recent review and stresses the influence of bubble interactions on the sound speed. A first integral of the motion has been established for potential flows of bubbly liquids in simple geometries (Wallis (1991)). The propagation of waves of moderate amplitude and the occurrence of shocks in one-dimensional bubbly flows have also been studied (e.g. van Wijngaarden 1980; Watanabe & Prosperetti 1994). Here there is a need to evaluate the effect of possibly large pressure changes in inhomogeneous two-dimensional bubbly flows. Since no simple approach seems possible in such configurations we resort to the crude assumption that the mixture behaves as a compressible fluid. The drastic assumption of no added-mass effect seems reasonable in the far end of the container and the incoming jet but is questionable around the stagnation point, O, where the existence of strong pressure gradients may induce high flow inhomogeneity. With the mass fraction of each constituent unchanged it might be expected that compressibility effects are most significant in that region of high pressure. However, subsequent results (§3.6) show that air is virtually eliminated in regions of high pressure so there is probably little error on this account.

3.2. *Conservation of mass and momentum flux*

Our basic assumption is that of no 'slip' velocity or relative translational movement between the phases. Therefore there is no dissipation caused by relative motion between the liquid and the bubbles and the mass flux of gas in a unit mass flux of the mixture is constant. With this assumption and using (3.1) it is straightforward to write equations for conservation of mass and momentum flux for a compressible mixture. Denoting by ρ_1 the density of the incoming mixture and by ρ its density in the far end of the container (see figure 1*b*), we have in dimensional form,

$$\rho U H = \rho_1 V_0 (h - d), \tag{3.2}$$

for mass conservation, and

$$\left(\rho U^2 + P - P_1\right) H = \rho_1 V_0^2 (h + d), \tag{3.3}$$

for momentum flux, where P_1 is the reference pressure (atmospheric pressure) in the incoming and outgoing mixture. In PK the pressure P_1 was ignored and results given as over pressures with respect to a zero pressure reference. Here, as in any compressible flow, P_1 is a central parameter. In (3.2) and (3.3) the densities ρ_1 and ρ may be expressed as the gas volume fraction weighted average of the gas and liquid densities, ρ_g and ρ_l, respectively:

$$\rho = \beta \rho_g + (1 - \beta)\rho_l, \tag{3.4a}$$

$$\rho_1 = \beta_1 \rho_{g1} + (1 - \beta_1)\rho_l. \tag{3.4b}$$

The subscript 1 always refers to standard conditions in the incoming jet. In equations (3.4*a*,*b*) we have assumed that the motion is violent but not so violent that we should allow for the compressibility of the water. Thus the liquid phase is taken as incompressible. The next approximation is to neglect the gas density compared to the liquid density, namely

$$\rho \simeq (1 - \beta)\rho_l, \tag{3.5a}$$

$$\rho_1 \simeq (1 - \beta_1)\rho_l. \tag{3.5b}$$

This is an excellent approximation for the air–water system for pressures up to 10 bar, and even over this limit for the small gas fractions considered here. Although a 'steady' flow is being considered we are assuming timescales in which there is negligible dissolution of the gas. Then use of (3.5) in (3.2) and (3.3) yields

$$(1 - \beta) U H = (1 - \beta_1) V_0 (h - d), \tag{3.6}$$

$$\left[\rho_l (1 - \beta) U^2 + P - P_1\right] H = \rho_l (1 - \beta_1) V_0^2 (h + d). \tag{3.7}$$

3.3. *State equation*

To evaluate substantial pressure changes it is desirable to choose a suitable pressure–density relation, or equation of state, for the mixture. This is similar to the approach used in gas dynamics. When considering water with a volume fraction of air β_1, we need to decide whether the air is contained inside very small bubbles that change volume in an isothermal manner or larger bubbles that behave adiabatically. A unifying approach, to take account of limited heat flow, is to assume that the gas changes volume according to the polytropic law

$$P_g \rho_g^{-\kappa} = \text{constant}, \tag{3.8}$$

with the polytropic index κ given intermediate values between $\kappa = 1$ (isothermal behaviour) and $\kappa = \gamma$ (adiabatic behaviour), where γ is the ratio of constant-pressure and constant-volume specific heats of the gas; $\gamma \simeq 1.4$ for air. For the time being we shall assume that $\kappa \simeq \gamma$. The rôle of the value of κ is addressed in §4.4.

To derive a state equation for a compressible air–water mixture, consider a given mass of mixture occupying an initial volume, $\mathscr{V}_1$, at reference pressure P_1. This volume contains a fraction $\beta_1\mathscr{V}_1$ of gas, and a fraction $(1-\beta_1)\mathscr{V}_1$ of liquid. At another ambient pressure, P, the mixture occupies a different volume, $\mathscr{V}$, but its mass is preserved; therefore,

$$\rho_1\mathscr{V}_1 = \rho\mathscr{V}, \tag{3.9}$$

where ρ_1 is the density of the mixture when the pressure is P_1 and ρ its density when the pressure is P. As stated earlier we take the liquid to be incompressible and the gas to change volume polytropically. Thus, the liquid volume is unchanged, but the gas now has volume $\beta_1\mathscr{V}_1(P_1/P)^{1/\kappa}$, according to (3.8). Hence, the new volume occupied by the mixture is

$$\mathscr{V} = (1-\beta_1)\mathscr{V}_1 + \beta_1\mathscr{V}_1\left(\frac{P_1}{P}\right)^{1/\kappa}. \tag{3.10}$$

Upon substituting (3.9) in (3.10), we arrive at the equation of state

$$\frac{1}{\rho} = \frac{1-\beta_1}{\rho_1} + \frac{\beta_1}{\rho_1}\left(\frac{P_1}{P}\right)^{1/\kappa}. \tag{3.11}$$

In deriving (3.11) the surface tension σ is neglected, whence the pressure in the gas bubbles and in the surrounding liquid are considered equal and represent the actual pressure in the mixture. The especially violent flows considered here have sufficiently high pressures compared with the Laplace pressure, $2\sigma/R_0$, that neglecting surface tension is a realistic approximation.

To simplify (3.11) a new variable,

$$\delta = 1 - \frac{\rho_1}{\rho}, \tag{3.12}$$

is introduced. Upon substituting (3.12) in (3.11) we get a compact expression for the equation of state

$$\frac{P}{P_1} = \left(\frac{\beta_1}{\beta_1 - \delta}\right)^{\kappa}, \tag{3.13}$$

which is useful in Bernoulli's equation. This equation is implicitly contained in van Wijngaarden (1972).

3.4. *Bernoulli's equation*

A compressible fluid in a steady inviscid flow satisfies Bernoulli's equation

$$\int \frac{\mathrm{d}P}{\rho} + \frac{1}{2}q^2 = \text{constant}, \tag{3.14}$$

where q is the magnitude of the velocity. Integration of the first term in the left-hand side of (3.14) yields, using (3.13),

$$\rho_1 \int_{P_1}^{P} \frac{\mathrm{d}P}{\rho} = P\left(1 + \frac{\beta_1 - \delta\kappa}{\kappa - 1}\right) - \frac{P_1\beta_1}{\kappa - 1} - P_1. \tag{3.15}$$

Note that (3.15) is singular when $\kappa = 1$, which corresponds to isothermal behaviour of the gas. For completeness isothermal expressions are given in the Appendix, but we continue in the following with the assumption that $\kappa \neq 1$.

For subsequent algebraic convenience equation (3.15) is rewritten in the form

$$(1-\beta_1)\int_{P_1}^{P}\frac{\mathrm{d}P}{\rho} = \left(\frac{P-P_1}{\rho_l}\right)\left[1-\beta_1\left(\frac{\kappa-1-\kappa\mu}{\kappa-1}\right)\right] - \frac{\kappa}{\kappa-1}\frac{\beta_1 P_1}{\rho_l}(1-\mu), \quad (3.16)$$

where μ is defined from the equation of state (3.13) as

$$\mu = \left(\frac{P_1}{P}\right)^{1/\kappa} = \frac{\beta(1-\beta_1)}{\beta_1(1-\beta)}. \quad (3.17)$$

In evaluating (3.16) and (3.17) we have neglected the gas density compared to the liquid density (see equation (3.5)) to be consistent with the mass and momentum conservation equations (3.6) and (3.7).

3.5. *Dimensionless equations*

The natural velocity scaling in a compressible flow is Mach scaling. However the aim of this paper is to appreciate compressibility effects in violent flows. This is achieved most directly by comparison with the incompressible solution. Consequently our choice is to normalize all velocities with the incoming jet velocity V_1 and the pressures with $\frac{1}{2}\rho_l V_1^2$. The height of the container H is the natural length scale. These choices are identical to those adopted in PK. We use small letters for dimensionless quantities (with the exceptions that d, h and densities are dimensional); these are

$$\left.\begin{aligned} &x = d/H,\ k^2 = h/H, \quad u = U/V_1, \quad v = V_0/V_1, \\ &p_1 = P_1/\left(\tfrac{1}{2}\rho_l V_1^2\right), \quad p = P/\left(\tfrac{1}{2}\rho_l V_1^2\right), \quad p_m = P_m/\left(\tfrac{1}{2}\rho_l V_1^2\right). \end{aligned}\right\} \quad (3.18)$$

The set of equations now consists of the non-dimensional kinematic condition (3.1*a*), mass conservation (3.6), momentum flux balance (3.7), Bernoulli's equation (3.14) applied between the incoming jet and the filled portion of the container making use of (3.16), and the state equation (3.17):

$$v - u = 1, \quad (3.19a)$$

$$(1-\beta)u = (1-\beta_1)\left(k^2 - x\right)v, \quad (3.19b)$$

$$2(1-\beta)u^2 + p - p_1 = 2(1-\beta_1)\left(k^2 + x\right)v^2, \quad (3.19c)$$

$$(p-p_1)\left[1-\beta_1\left(\frac{\kappa-1-\kappa\mu}{\kappa-1}\right)\right] = \frac{\kappa}{\kappa-1}\beta_1 p_1(1-\mu) + (1-\beta_1)\left(v^2-u^2\right), \quad (3.19d)$$

$$\mu = \left(\frac{p_1}{p}\right)^{1/\kappa} = \frac{\beta(1-\beta_1)}{\beta_1(1-\beta)}. \quad (3.19e)$$

A further equation is needed to get the maximum pressure p_m at the stagnation point. This is obtained with Bernoulli's theorem and the state equation applied between the stagnation point and the incoming jet:

$$p_m - p_1 + \left(\frac{\kappa}{1-\kappa}\right)\left(\frac{p_1\beta_1}{1-\beta_1}\right)\left[1-\left(\frac{p_m}{p_1}\right)^{1-1/\kappa}\right] = v^2. \quad (3.19f)$$

The set of equations (3.19) is solved for x, β, u, v, p, and p_m once the inflow parameters, i.e. k, β_1, P_1, and V_1, are prescribed. A Newton iteration initialized with the incompressible solution plus β initialized as β_1 is sufficient for that purpose.

3.6. *Approximate solution*

As well as the small parameter ρ_g/ρ_l which we have already used, there are two further small parameters in this problem: the clearance of the incoming flow

$$\epsilon = (H-h)/H = 1-k^2, \tag{3.20}$$

and the volume fraction of air bubbles β_1. These enable approximate solutions to be found which give some insight into the cushioning effect of the entrained air.

First, we consider the approximate solution to the incompressible flow to clarify the subsequent compressible analysis. Although for violent examples the incompressible solution (2.1) indicates that $1-k$ is the relevant small parameter, we use ϵ as the small parameter for algebraic simplicity. The variables u, v, $p-p_1$ are all $O(1/\epsilon)$ whereas x is $O(\epsilon^2)$. The relative velocity condition, $v-u=1$, permits simplification of the incompressible Bernoulli's equation:

$$p-p_1 = v^2-u^2 = v+u. \tag{3.21}$$

The mass and momentum conservation equations can also be simplified to give

$$v-u = v(\epsilon+x) = 1, \tag{3.22}$$

$$v+u = 2v^2(\epsilon-x) = 2v-1, \tag{3.23}$$

respectively, where the right-hand side of (3.23) follows from the relative velocity condition.

For $\epsilon \ll 1$ it is clear that even for a first approximation one must include the second-order terms or the effect of the input flow V_1, corresponding to the the right-hand side of (3.22), does not appear. Further exact algebra leads to quadratic equations in v, u or x, but in (3.22) x can be neglected to give the first approximation $v = 1/\epsilon$, which is consistent with the leading-order terms in (3.23). Thus, as may be seen from PK, to the first order in ϵ the filled pressure is the same for both the filling flow with a small return jet, PK equation (8), and the case without return jet that includes turbulent dissipation, PK equation (14). We also note that to find x the next approximation to v is necessary.†

We now return to the compressible flow. The set of equations to be approximated is (3.19). Upon using (3.19*a*) and rearranging terms, (3.19*b*) becomes

$$v\left[\frac{\epsilon+\beta_1-\beta-\epsilon\beta_1+(1-\beta_1)x}{1-\beta}\right] = 1, \tag{3.24}$$

similar to (3.22). Using (3.19*d*) to eliminate the pressure difference $p-p_1$ and looking for similarity to (3.23), equation (3.19*c*) becomes

$$\begin{aligned} 2v-1 = {} & \frac{2v^2}{\alpha}\left[\beta_1-\beta+\epsilon-\beta_1(\epsilon-x)-x\right] \\ & + \frac{2\beta}{\alpha}(2v-1) + \left(\frac{\kappa}{\kappa-1}\right)\left(\frac{p_1\beta_1}{1-\beta_1}\right)\left(\frac{2-\alpha}{\alpha}\right)(1-\mu), \end{aligned} \tag{3.25}$$

where

$$\alpha = 2 - \frac{(1-\beta_1)(\kappa-1)}{(1-\beta_1)(\kappa-1)+\beta_1\kappa\mu}. \tag{3.26}$$

† The next approximation has solution $v = \epsilon^{-1}(1-\frac{1}{4}\epsilon+O(\epsilon^2))$, $u = \epsilon^{-1}(1-\frac{5}{4}\epsilon+O(\epsilon^2))$, $p-p_1 = 2\epsilon^{-1}(1-\frac{3}{4}\epsilon+O(\epsilon^2))$, $p_m-p_1 = \epsilon^{-2}(1-\frac{1}{2}\epsilon+O(\epsilon^2))$, $x = \frac{1}{4}\epsilon^2+O(\epsilon^3)$, consistent with the exact solutions of PK.

To evaluate leading-order terms in (3.25) we need an order of magnitude for μ. This is obtained from the state equation (3.19*e*), from which we infer that

$$\mu = O\left(\beta/\beta_1\right) = O\left(\epsilon^{1/\kappa}\right). \tag{3.27}$$

Thus, we deduce that $\alpha = 1 + O(\beta_1\epsilon^{1/\kappa}, \beta_1^2)$. Correct to first order, either (3.25) or (3.24) give the same approximation:

$$\frac{1}{v} \simeq \epsilon + \beta_1 - \beta \simeq \epsilon + \beta_1(1-\mu) + O\left(\beta_1\epsilon, \beta_1^2, \epsilon^2\right). \tag{3.28}$$

Using (3.27) one may further approximate

$$v = \frac{1}{\epsilon + \beta_1 + O(\beta_1\epsilon^{1/\kappa})}. \tag{3.29}$$

At this level of approximation we are effectively assuming that air is of negligible volume at high pressure since $\mu \ll 1$ when ϵ is small enough. The filling and maximum pressures are, to the same level of approximation,

$$p - p_1 = \frac{2}{\epsilon + \beta_1}, \text{ and } p_m - p_1 = \frac{1}{(\epsilon + \beta_1)^2}. \tag{3.30}$$

This first-order solution clearly shows how the gas fraction β acts to cushion the pressures, with the maximum pressure being cushioned as the square of the filling pressure. Futher, the absence of κ shows that only the volume change is significant in this approximation.

The next approximation is needed to find x. Note however that the algebra becomes difficult since nonlinear terms of $O(\beta_1\epsilon^{1/\kappa})$ must be kept in the next approximation, and this is taken no further here. Approximate first-order results are compared to exact numerical calculations in §4.3.

4. Results

4.1. *Prescription of the inflow*

There are two kinds of parameters defining the incoming flow. First ϵ determines the violence of the flow. This is an incompressible parameter as it is defined independently of the air content. There are three other parameters driving the compressibility of the incoming mixture. These are the atmospheric or equilibrium pressure P_1, the velocity V_1, and the air fraction β_1. We choose a constant atmospheric pressure $P_1 = 1$ bar so that only V_1 and β_1 are left free. The maximum value used for β_1 is 0.10 since a number of our assumptions become poor for non-dilute dispersions. The range of values for the incoming velocity V_1 remains to be determined. For this purpose we note that the three parameters P_1, V_1, and β_1 uniquely define the speed of sound in the bubbly mixture. Small-amplitude disturbances in a bubbly mixture travel at a speed (e.g. Hsieh & Plesset 1961)

$$C_1 = \left[\frac{\kappa P_1}{\rho_l \beta_1 (1-\beta_1)}\right]^{1/2}. \tag{4.1}$$

This quantity appears naturally in Bernoulli's equation but was not chosen to scale velocities in (3.19) for reasons explained in §3.5. Expression (4.1) is now useful to choose the range of V_1. With $\beta_1 = 0.10$ and $P_1 = 1$ bar, the minimum sound speed in the mixture is $C_1 = 33\ \mathrm{m\,s^{-1}}$. In the following we choose values of V_1 between 1

and 10 m s^{-1}. In using this range of velocity the incoming jet can be viewed as due to a water wave whose height varies between a few centimetres (typical of small-scale experiments in the laboratory) and a few metres (typical of a field situation). In this parameter range the incoming Mach number $\mathscr{M}_1 = V_1/C_1$ seen in the fixed frame of reference is subsonic. Therefore the deceleration of the fluid between the incoming jet and the filled portion of the container occurs without shock formation. However the filling-velocity Mach number ($\mathscr{M} = V_0/C_1$) seen in the moving frame can be supersonic because U is much larger than V_1 in sufficiently violent flows. In the most severe cases we found $\mathscr{M}$ between 1.2 and 2.

The return jet may be supersonic in the reference frame of the container for significantly less violent flows, but it seems unlikely that this would of itself cause shock waves in the transonic flow. For supersonic advance of the filled region, relative to the incoming flow, it is clear that a smooth flow such as described in figure 1 is not possible. Shock formation is likely and return flow is unlikely. Thus the overall flow behaviour is dissipative and the pressure in the filled portion can be found from mass and momentum conservation, as at the end of §3 in PK. The results for the background pressure differ very little from those calculated from equations (3.19), as may be deduced from the approximate solution in §3.6. Whenever necessary those flows which are supersonic are indicated by using a broken line in the figures hereafter. The pressure maximum is assumed to be absent and is not shown. The absence of a pressure peak implies a significant reduction in force: but see §6 for some further discussion related to wave impact.

4.2. *Influence of the violence of the flow*

The results presented here are for air changing volume adiabatically, $\kappa = \gamma$. They are presented as 'compressibility reduction factors'. For example, figure 2(*a*) shows the background pressure $p(\beta_1)$ that develops in the filled portion of the container as a function of β_1. The pressure has been normalized with the pressure $p(\beta_1 = 0) = p^{(i)}$ of the corresponding incompressible flow, i.e. the ratio $p(\beta_1)/p^{(i)}$ is plotted. Four curves are plotted, each one corresponding to a different clearance, ϵ. The velocity of the incoming jet is here $V_1 = 8$ m s^{-1}. There is little compressible effect on the pressure p when the motion is not very violent, i.e. for ϵ not so small. As one should expect, the compressibility effects are more prominent in more severe flows. When $\epsilon = 0.19$, p is decreased by 15% for 5% volume fraction of air in the incoming flow. In a more extreme case, $\epsilon = 0.10$, compressibility reduces p by 25% for the same value of β_1. The cushioning effect of air is even stronger as regards the maximum pressure p_m at the stagnation point. With $\beta_1 = 0.05$ the corresponding values of p_m when $\epsilon = 0.19$ and 0.10 are decreased by 20% and 50%, respectively. The fact that the maximum pressure is reduced more than the background pressure in severe flows is clearly demonstrated in the approximate solution (3.30).

Notice that the discontinuity in filling pressure where $\mathscr{M}$ becomes supersonic is small. This is consistent with the approximate solution which predicts that results with or without a return jet are the same to first order (see §§3.6 and 4.3 hereafter). Another point worth mentioning is that $\mathscr{M}$ becomes supersonic for very small values of air fraction when the flow is especially violent.

Another way to vary the violence of the flow is to change the inflow V_1, keeping ϵ fixed. Results are presented in figures 3(*a*) and 3(*b*) for the fixed value $\epsilon = 0.10$. These figures are particularly illustrative since they show that the pressures are not cushioned at lower velocity (i.e. in small-scale flows) whereas they are significantly cushioned at the higher velocities (i.e. in large-scale flows). These results are better understood

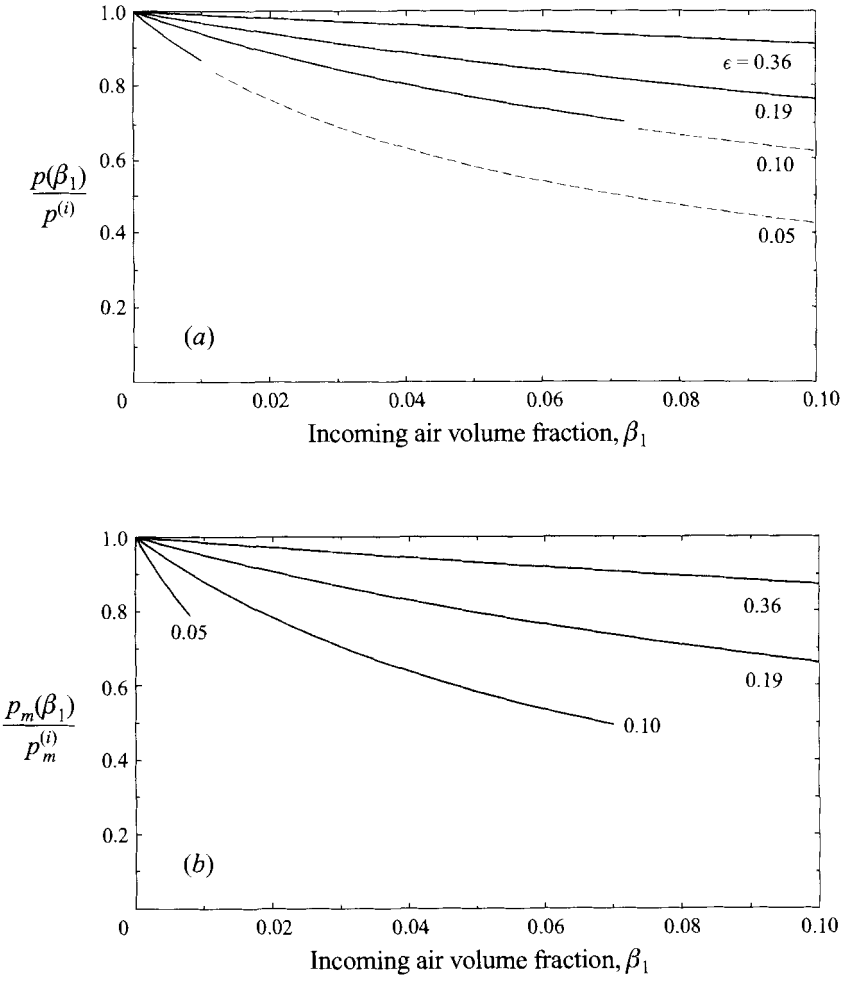

FIGURE 2. Pressure reduction factors as a function of β_1, $V_1 = 8\ \mathrm{m\,s^{-1}}$: (*a*) background pressure p and (*b*) maximum pressure p_m; dashed lines indicate where the 'filling' velocity Mach number $\mathscr{M} = V_0/C_1$ becomes supersonic.

when considering the inflow Mach Number $\mathscr{M}_1$. For the slow inflow in figures 3(*a*) and 3(*b*) the maximum value of $\mathscr{M}_1$, occurring for $\beta = 0.10$, is 0.05 whereas for the fast inflow $\mathscr{M}_1$ reaches 0.20. The reader familiar with compressible flows may be astonished to find pronounced compressibility effects in flows with moderate incoming Mach numbers. For instance the air flow in a convergent–divergent pipe is often considered incompressible for Mach numbers as high as 0.30. However it must be kept in mind that the flows considered here are violent with a wide range of velocities. This is the reason why the pressures are decreased so much even at moderate Mach numbers.

4.3. *Approximate results*

Examples of background and maximum pressure reduction factors computed exactly are plotted in figures 4(*a*) and 4(*b*) together with the corresponding approximate solution presented in §3.6. The incoming velocity is here $V_1 = 10\ \mathrm{m\,s^{-1}}$. Curves here are not interrupted when $\mathscr{M} > 1$ to allow comparison on the whole range of air

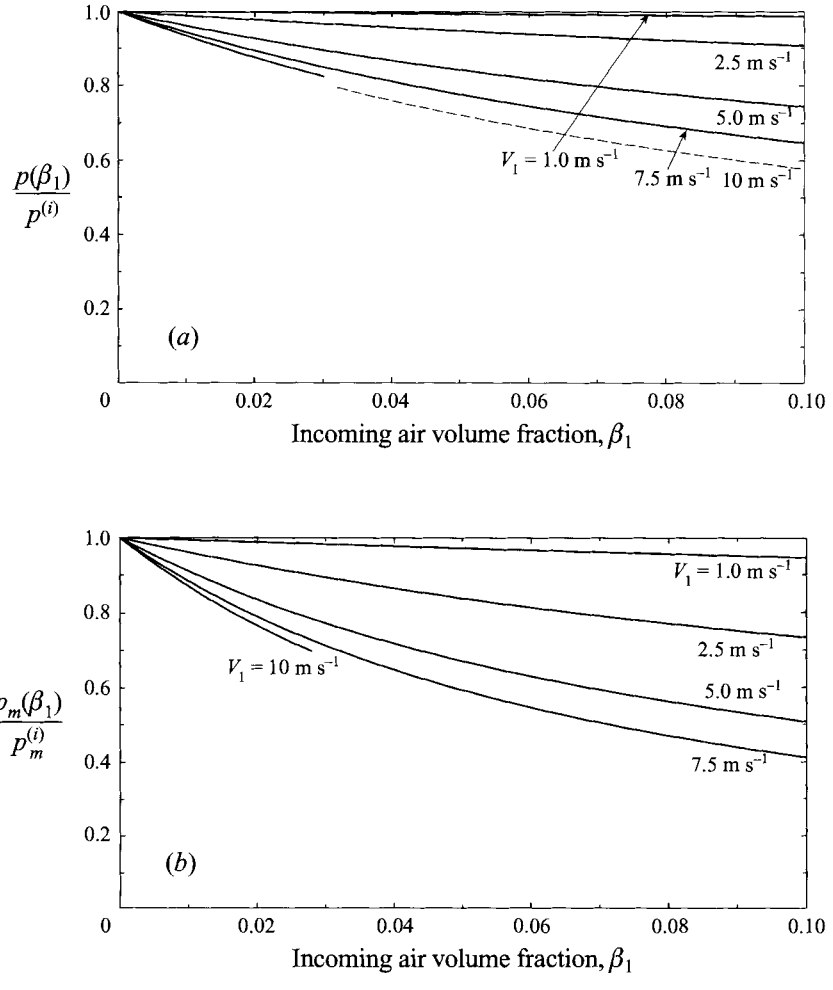

FIGURE 3. Pressure reduction factors as a function of β_1 for various inflows V_1 and $\epsilon = 0.10$: (*a*) background pressure p and (*b*) maximum pressure p_m; dashed lines indicate where the 'filling' velocity Mach number $\mathscr{M} = V_0/C_1$ becomes supersonic.

volume fraction. Figure 4(*a*) is for a violent flow where $\epsilon = 0.05$. Results compare reasonably well in this case. Figure 4(*b*) is for the same incoming velocity but a less violent flow where $\epsilon = 0.19$. The results do not compare so nicely in that case because ϵ is not small enough. Note that the approximate reduction factors can be larger than 1 because these have been normalized with the exact results for the incompressible pressures. This choice allows us to see the error due to the approximation for small air content. We can estimate the error involved in the approximate solution. For small air content we deduce from the incompressible solution correct to $O(\epsilon^2)$ that the error in $p - p_1$ is of order $3\epsilon/4$. This corresponds to errors of 4% and 15% when ϵ equals 0.05 and 0.19, respectively. When the air content is larger the error is $O(\beta_1\epsilon^{1/\kappa} + \beta_1\epsilon)$. For $\beta_1 = 0.10$, these errors are found to be 0.6% and 5% when ϵ equals 0.05 and 0.19, respectively. These order of magnitudes correspond roughly to the differences seen in figure 4. The approximate solution is therefore an efficient way to get a rough estimate of the cushioning effect in practical applications.

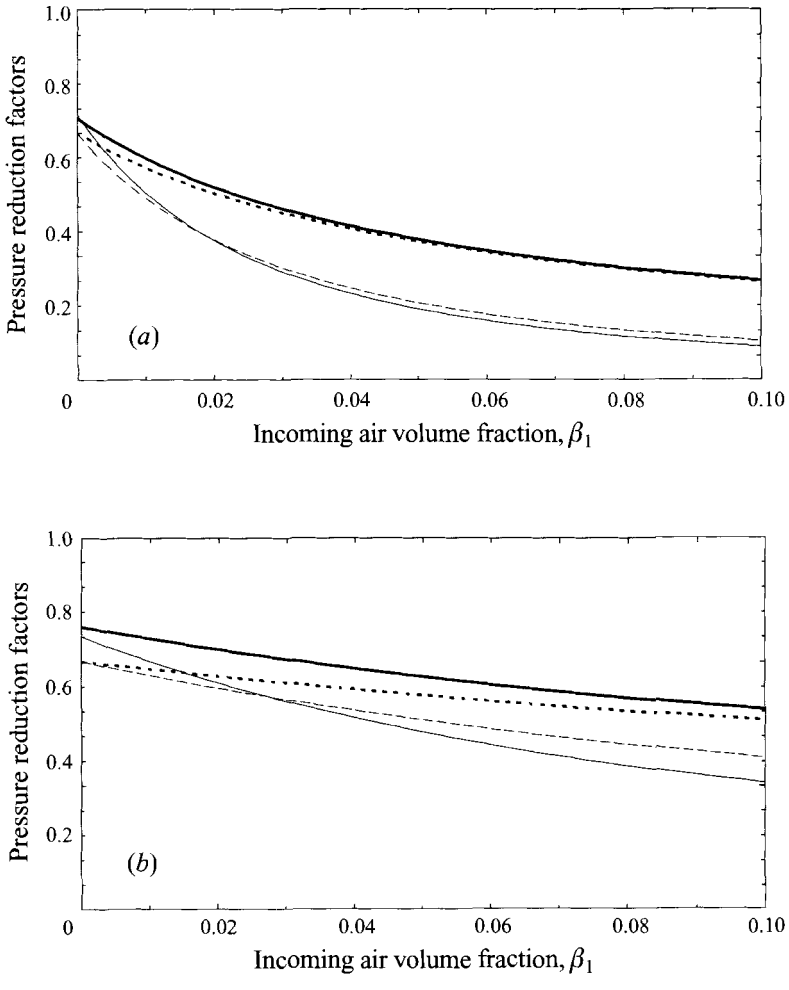

FIGURE 4. Approximate and exact solutions for the background and maximum pressure reduction factors: (*a*) $\epsilon = 0.05$, $V_1 = 10\ \mathrm{m\,s^{-1}}$ (*b*), $\epsilon = 0.19$, $V_1 = 10\ \mathrm{m\,s^{-1}}$; ——, approximate background pressure; - - - -, exact background pressure; ———, approximate maximum pressure; – – –, exact maximum pressure. Curves here are not interrupted when $\mathscr{M} > 1$ to allow comparison on the whole range of air volume fraction.

4.4. *Influence of the polytropic index* κ

The question of the influence of the polytropic index κ has been left unanswered in §3. The radius of a typical bubble is in the range 0.1 to 1 mm either in breaking waves near the shore (Leighton 1994, p. 215) or during artificial injection of air in a water column (Scott 1975). It is not clear whether adiabatic or isothermal compression should dominate in this size range. We have therefore studied the sensitivity of the results to the value of κ. Results presented here are for the violent flow where $\epsilon = 0.10$ and an incoming jet velocity $V_1 = 8\ \mathrm{m\,s^{-1}}$. Nonetheless similar results hold for all the flows we have examined. Figure 5 portrays the maximum-pressure reduction factor for five different values of κ, namely $\kappa = 1$ (isothermal), 1.1, 1.2, 1.3, and γ (adiabatic). In general, there is very little difference between each plot in figure 5. The maximum discrepancy in p_m is only 0.02 between adiabatic and isothermal compression. Note that the lowest maximum-pressure reduction factor is

obtained for isothermal compression. There is even less discrepancy in the results for the background pressure (not shown here). However, κ does have a significant effect on the velocity of sound, so the supersonic regime occurs for less violent flows as κ is reduced. This implies that exceptionally small bubbles, which correspond to low κ, may have a greater effect in limiting maximum pressures.

The approximate solution presented in §3.6 helps us understand why results depend little on the value of the polytropic index. To first order, the approximate solution (3.30) for the pressure reductions is independent of κ. This is an expected feature since (3.30) just assumes that air is eliminated at high pressure.† It is helpful that the pressure reductions depend little on κ. This allows an accurate computation of the cushioning effect whatever the actual value of κ, a quantity rather difficult to estimate in practice. For bubbles in the size range considered here it is likely that an adiabatic compression in the first place would be followed by a decrease in κ, resulting in a final isothermal equilibrium (with the proviso that the liquid be viewed as a large isothermal reservoir). Owing to the small sensitivity of the results to a constant value of κ, we believe that taking into account this unsteady heat transfer would have little effect on the pressure reductions. Watanabe & Prosperetti (1994) point out that for unsteady pressure fields a simple equation of state is inappropriate. This is due to the forcing of bubble oscillations. Whether or not this is important here is not clear, but the insensitivity to the details of the equation of state demonstrated in figure 5 gives us some confidence in our results.

The lack of sensitivity to the precise equation of state is also reassuring when considering the effects of bubble motion relative to the water. Since bubbles have no significant inertia other than their added mass, they have a very strong response to pressure gradients. This can lead to fewer bubbles in the regions of highest pressure as preliminary computations of bubble trajectories demonstrate. However, since we see that in these regions the bubbles have a nearly negligible volume fraction, bubble migration can be expected to have little effect on these results. Aspects of bubble migration are being studied further.

5. Discussion and application to flip-through

We have emphasized in this paper how a small fraction of air dispersed as bubbles in water can significantly lower the high pressures encountered in violent confined flows. Such differences between compressible and incompressible flows are not surprising. Even a small fraction of air dramatically lowers the sound speed. Therefore Mach numbers based on this sound speed can reach significant values in large-scale flows. The rôle of compressibility as described here is applicable to substantial changes of pressure whereas sound speed relates to small or moderate perturbations. Another point of especial interest is that these results are for an unsteady flow. Although the analysis makes use of a frame of reference in which the flow is steady the velocity of the reference frame, U, depends on the incoming air content. The approximate solution of §3.6 sheds light on this mechanism. Equation (3.29) shows that V_0 and U are reduced as the air content increases. This reduction in the velocity of filling is a consequence of the effective volume of the fluid being reduced at high pressure.

The simplicity of these results suggests that they may be suitable for application

† The approximate solution for exactly isothermal compression ($\kappa = 1$) is identical to (3.30). This is due to the fact that the first-order expansion in the isothermal Bernoulli's equation (A 2) is identical to the first-order expansion of (3.19*d*)

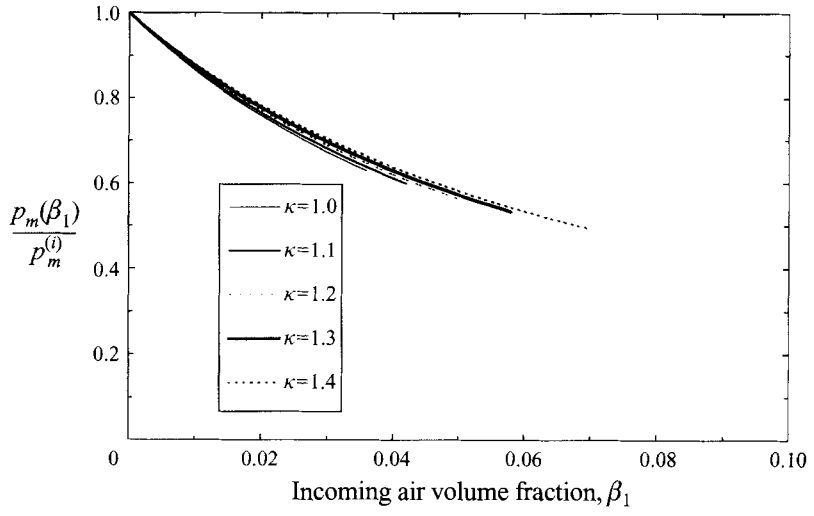

FIGURE 5. Influence of the polytropic index κ on the maximum pressure; $\epsilon = 0.10$, $V_1 = 8\ \mathrm{m\,s^{-1}}$; curves are interrupted where the filling velocity Mach number becomes supersonic ($\mathscr{M} > 1$).

in other circumstances, the flip-through type of wave impact being the most directly relevant. Figure 6 shows a pressure distribution on the 'upper' wall for a filling flow, using the complete two-dimensional incompressible solution found by PK, together with a pressure distribution on a vertical wall due to a flip-through wave impact computed with a full potential flow description (Cooker & Peregrine (1996)). Similar quantities have been chosen to scale both length and pressure. The distance x along the wall has been normalized with the distance between the point of maximum pressure and the point on the free surface with tangent perpendicular to the wall. The pressure for the flip-through has been normalized using density and the difference between the velocity of the jet and the velocity of the maximum pressure point. For the filling flow the pressure has been normalized with the jet velocity V in the moving frame of reference. The parameter k for the incompressible filling flow was chosen to match the ratio $R = p_m^{(i)}/p^{(i)}$ between the maximum and background pressure for the flip-through. Here the background pressure is taken to be that near the bed ($x \simeq -80$, in figure 6). From equations (2.1*a*,*b*) the appropriate value of k is given by

$$k = \frac{1}{2}\left[1 + \left(\frac{R-1}{R}\right)^{1/2}\right]. \tag{5.1}$$

In the example chosen for figure 6 the background pressure is about one sixth of the maximum pressure and so $k = 0.96$. Given the considerable differences in the two flow fields, one in a narrow channel, the other in a quarter-plane, the similarity of the pressure distributions in figure 6 is very encouraging. Both have the same general trend with the two major discrepancies being that in the flip-through profile shown the pressure maximum is 25% higher and the pressure reaches its background value more quickly. Other computations of flip-through waves have provided dimensionless maximum pressures between 0.8 and 1.3. In a filling flow the pressure relaxes to its background value more slowly because the background pressure is asymptotically reached at infinity while the flip-through is in a less confined domain.

We now proceed to explain how our results might be used in practice. The

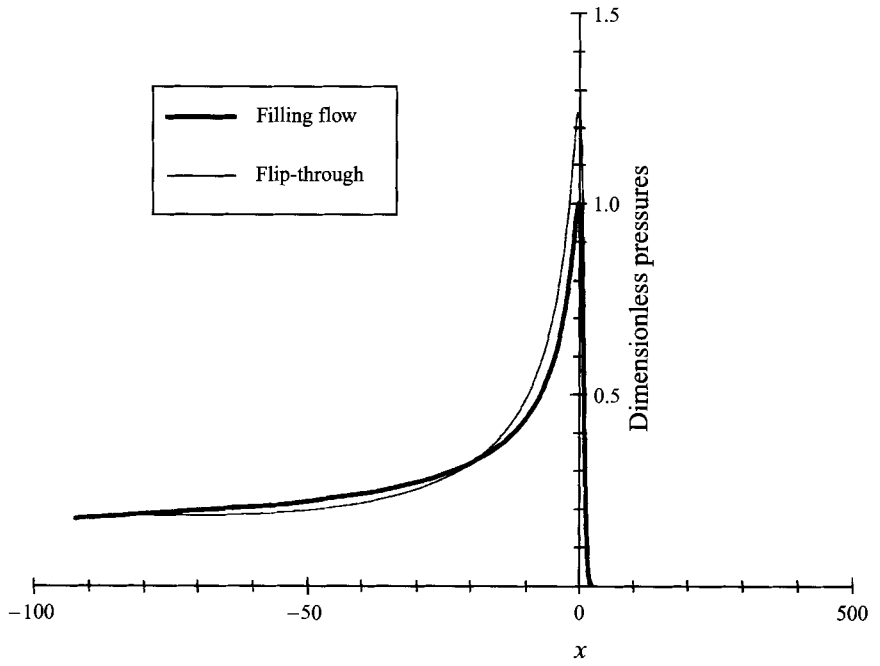

FIGURE 6. Dimensionless pressures observed on the 'upper' wall in a filling flow and on the vertical wall in a flip-through.

reductions in pressure due to entrained air shown in figure 2 are not uniform. The peak is reduced more than the 'background' pressure. Although, at first, this appears to make it difficult to apply our results, the similarities in figure 6 and consideration of how such values are used gives a different view.

Many, if not all, applications of wave impact forces in design calculations rely on a simplified pressure distribution, e.g. that of Goda (1974). These are described by few parameters, which are easy to modify in line with pressure variations of the type shown in figure 2.

The engineer is faced with the problem of scaling pressures measured in small-scale laboratory experiments to larger scales in the field. Suppose that we know the dimensional values of the background and maximum incompressible pressures, P and P_m, quantities which are accessible from pressure gauges fitted on the wall of a laboratory tank. Computation of the pressure reductions due to compressibility requires knowledge of a typical incoming velocity V_1 in the large-scale flow. For instance V_1 may be inferred from knowledge of the wave climate. For our purpose we choose $V_1 = 8\ \mathrm{m\,s^{-1}}$. Following the method outlined in §3 further diagrams of the exact results for adiabatic compression are given in figures 7(*a*) and 7(*b*) to assist. In these the incompressible pressure, $p^{(i)}$ or $p_m^{(i)}$, is this time used as the input variable and each curve corresponds to a unique value of β_1.

However, these pressures are normalized with a reference pressure P_R, say. To use figure 7, P_R must be found. If the approach velocity of the wave in the small-scale experiment, say V_{s1}, is known, then we have $P_R = \frac{1}{2}\rho_l V_{s1}^2$. Alternatively, if the speed V_{s1} is not known from experiments the reference pressure P_R may be inferred from the dimensional values of the background and maximum incompressible pressures, P and P_m. As these are measured in a small-scale experiment, where little compressibility

effect is expected, we may use the incompressible solution of PK. When k is eliminated from the pair of equations (2.1*a*,*b*), and the dimensional pressures are inserted the following equation is found for P_R:

$$P_R^2 - 2(2P_m - P)P_R + P^2 = 0. \tag{5.2}$$

Solving the quadratic and choosing the value of P_R which is less than the other two pressures yields

$$P_R = 2P_m - P - 2[P_m(P_m - P)]^{1/2}. \tag{5.3}$$

The dimensionless values for $p = P/P_R$ and $p_m = P_m/P_R$ are then available for using figures 7(*a*) and 7(*b*) to give an estimate of the pressure reduction factors due to entrained air in water wave impact.

Finally we may take a numerical example to illustrate the theory. Typical pressures measured in the laboratory by Hattori & Arami (1992) are $P_m = 300$ cm of water, and $P = 60$ cm of water. Thus (5.3) gives $P_R = 3.3$ cm of water and the dimensionless pressures are $p = 18$, $p_m = 90$. For a prototype flow with $V_1 = 8\ \mathrm{m\,s^{-1}}$ and air content $\beta_1 = 0.05$, figure 7 tells us that the background pressure is reduced by 25%, whereas the maximum pressure is reduced by 45%.

6. Supersonic flow at impact

In the previous section supersonic flows, i.e. when $\mathscr{M} > 1$, are indicated in figure 7(*a*) by dashed lines, and in figure 7(*b*) by the premature termination of the lines. Once $\mathscr{M} > 1$ the flow pattern is no longer as shown in figure 1, and at wave impact a flip-through with rising jet is unlikely to occur. For the filling flow we have been unable to deduce any viable steady flow pattern when the filled region advances onto the incoming flow at supersonic speed. However, for a flip-through type of wave impact the general outline of a transonic flow pattern is more readily deduced. This is because the rising jet has strong similarities to the backward jet that occurs when two plane jets meet symmetrically at an oblique angle (Birkhoff *et al.* 1948). The corresponding conical flow leads to the Munroe jet that has been used in armour-piercing munitions. The two-dimensional problem of interest here has been studied by Walsh, Shreffler & Willig (1953), and may be extended to the wave impact case.

Consider the flow at a wall when a wave causes a flip-through. As the front of the wave comes close to the wall the point where the free surface meets the wall starts to move with violent acceleration, and for incompressible flow the highest pressures occur just as a thin high-speed jet forms. Now, if the contact-point velocity exceeds the sonic speed in the bubbly mixture no jet can form. Consideration of Walsh et al.'s solution shows that a shock forms at the contact point, extending into the fluid at the angle necessary to deflect the flow of the undisturbed face of the wave so that it becomes parallel to the wall. That is the flow behind the shock is made up of water that was in the face of the wave but is now rising up the wall at supersonic speed. Sketches of a flip-through and the corresponding compressible flow are shown in figure 8. The local configuration at the contact point is governed at any instant by the angle between the wall and the front face of the wave and the velocity of motion of the contact point. This is in fact the reverse of the transition that occurs from supersonic to subsonic flows when a liquid mass makes a direct impact with a solid, e.g. see Korobkin (1996) for a discussion. The shape of the shock will reflect the changing Mach number of the contact point and two possibilities for accelerating contact points are sketched in figure 8.

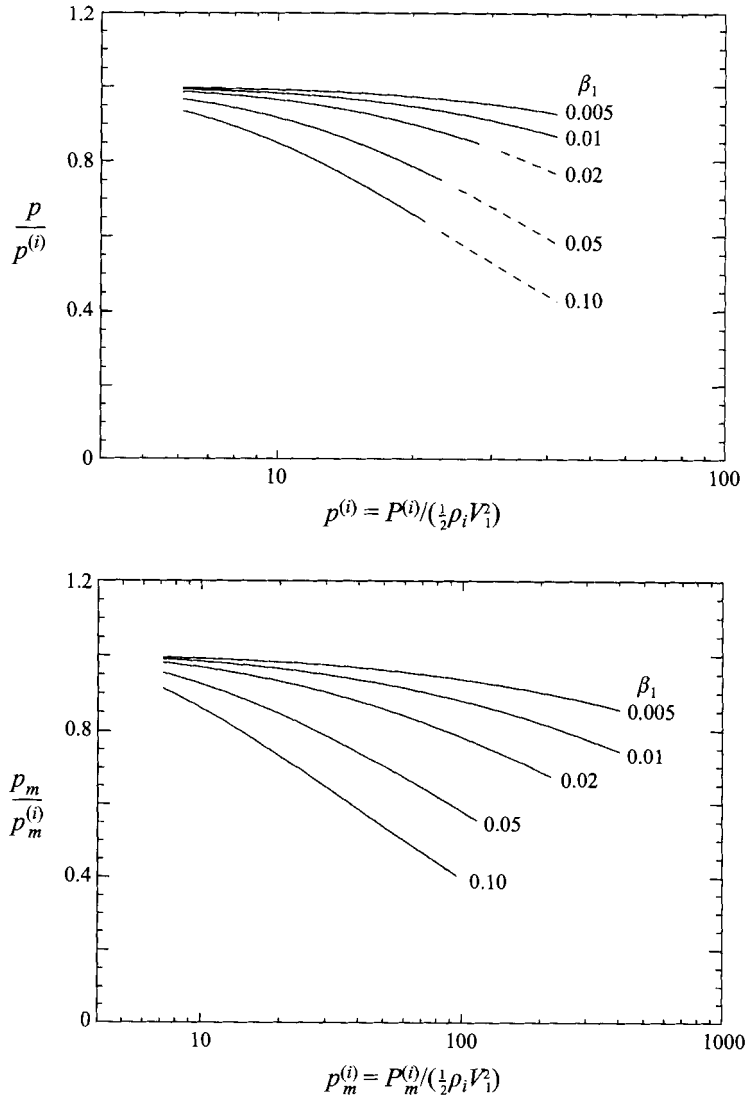

FIGURE 7. Pressure reduction factors for different values of the incoming air volume fraction β_1 as a function of normalized incompressible pressures, $V_1 = 8\ \mathrm{m\,s^{-1}}$: (*a*) background pressure $p^{(i)}$ and (*b*) maximum pressure $p_m^{(i)}$; dashed lines indicate where the 'filling' velocity Mach number $\mathscr{M} = V_0/C_1$ becomes supersonic.

The pressure rise at the shock can be deduced from the conservation of mass and momentum, and the fluid's equation of state. We do not follow through the analysis here, as in Walsh *et al.* (1953), for three reasons. Firstly, the angle between the free surface and the contact point is likely to change markedly. Secondly, the solution fails if the wave surface becomes parallel to the wall. Finally, bubbly fluids are likely to have significant shock structure, e.g see Watanabe & Prosperetti (1994) for a recent discussion. On the other hand, the configuration is worthy of deeper study since in the cases considered by Walsh *et al.* (1953), i.e. sheets of aluminium, iron and lead, the maximum pressures for a given velocity normal to their surfaces, i.e. before consideration of velocities relative to the contact point, occurred at the critical angle

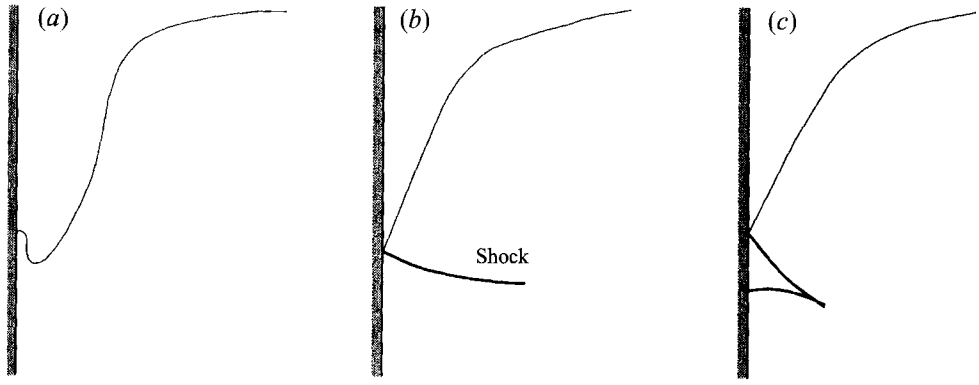

FIGURE 8. Sketches of wave impacts: (*a*) flip-through; (*b*) and (*c*) two different supersonic impacts with small and large contact point accelerations, respectively.

when shock formation only just occurred, whereas the minimum overpressure was that of the direct impact. Perhaps this is related to the disappearance of the maximum 'stagnation point' pressure. These topics are left for future study.

7. Conclusion

This paper provides a method to estimate the cushioning effect of air in violent free-surface flows. Expressions are formally derived for the filling flow of PK and results extrapolated to the flip-through wave impact. In using this approach it should be borne in mind that our arguments are based on a flow where air is dispersed as small bubbles rather than one that traps a large pocket of air. It is demonstrated that the background and maximum pressure reductions can be very large in spite of small volume fraction of air ($\beta_1 \leqslant 0.10$). The pressures decrease with increasing wave Mach number based on the sound speed in the air–water mixture and with the violence of the flow. Small-scale waves (low incoming velocity) show no significant cushioning of the pressures. Large-scale waves (fast incoming velocity) may have the maximum pressure they induce on a wall reduced by almost an order of magnitude, perhaps even more so if supersonic velocities are attained.

An approximate solution is derived for violent flows assuming that air is eliminated at high pressure. This simple argument shows that the maximum pressure is reduced as the square of the background pressure which itself is reduced because the reduced volume of the compressed mixture gives a lower filling velocity U. There is good agreement between the approximate solution and the exact numerical solution.

In practical applications it may be of primary importance to get a good estimate of β_1, the volume fraction of entrained air, to compare our estimates with experiments. Practically no field measurements are available, but work at Plymouth University is in progress making such measurements on a large breakwater. To conclude, the arguments presented here are likely to be relevant to other types of flows where large pressures occur that could be cushioned in the same way. The problem of ship slamming seems particularly pertinent.

Financial support is gratefully acknowledged from the Commission of the European Communities, Directorate General for Science, Research and Development under MAST Contracts MAS2-CT92-0047, MAS2-CT94-5025, MAS3-CT95-0041 and from the U.K. Engineering and Physical Sciences Research Council, Grant GR/H/96836.

Appendix. Bernoulli's equation for isothermal change of volume

The integral in Bernoulli's equation in §3 has been evaluated for non-isothermal change of volume of the gas ($\kappa \neq 1$). The corresponding calculation when $\kappa = 1$ induces a logarithm. The dimensional result reads

$$\int_{P_1}^{P} \frac{\mathrm{d}P}{\rho} = \frac{P - P_1}{\rho_l} + \frac{P_1}{\rho_l} \frac{\beta_1}{1 - \beta_1} \ln\left(P/P_1\right). \tag{A 1}$$

Thus the dimensionless Bernoulli's equation applied between the incoming flow and the filled portion of the container is

$$p - p_1 + \frac{\beta_1 p_1}{1 - \beta_1} \ln\left(p/p_1\right) = v^2 - u^2. \tag{A 2}$$

The additional equation necessary to compute the maximum pressure in the container is

$$p_m - p_1 + \frac{\beta_1 p_1}{1 - \beta_1} \ln\left(p_m/p_1\right) = v^2. \tag{A 3}$$

For isothermal change of volume equations (3.19*d*) and (3.19*f*) are to be replaced by (A 2) and (A 3), respectively, and κ must be set equal to 1 in (3.19*e*).

REFERENCES

BAGNOLD, R. A. 1939 Interim report on wave-pressure research. *J. Inst. Civil Engng*, **12**, 202–226.

BIRKHOFF, G., MACDOUGALL, D. P., PUGH, E. M. & TAYLOR, G. I. 1948 Explosives with lined cavities. *J. Appl. Phys.* **19**, 563–582.

COOKER, M. J. & PEREGRINE, D. H. 1990*a* Computations of violent motion due to waves breaking against a wall. *Proc. 22nd Intl. Conf. Coastal Engng, Delft*, vol. 1, pp. 164–176. ASCE.

COOKER, M. J. & PEREGRINE, D. H. 1990*b* A model for breaking wave impact pressures. *Proc. 22nd Intl. Conf. Coastal Engng, Delft*. ASCE. **2**, 1473–1486.

COOKER, M. J. & PEREGRINE, D. H. 1992 Wave impact pressure and its effect upon bodies lying on the bed. *Coastal Engng*, **18**, 205–229.

COOKER, M. J. & PEREGRINE, D. H. 1996 Computations of water wave impact on a wall and flip-through. In preparation.

GODA, Y. 1974 A new method of wave-pressure calculation for the design of composite break-water. *Proc. 14th Coastal Engng Conf. Copenhagen*, vol 3, pp. 1702–1720. ASCE.

HATTORI, M. & ARAMI, A. 1992 Impact breaking pressures on vertical walls. *Proc. 21st Intl Conf. Coastal Engng, Venice*, vol. 2, pp. 1785–1798. ASCE.

HSIEH, D.-Y. & PLESSET, M. S. 1961 On the propagation of sound in a liquid containing gas bubbles. *Phys. Fluids.* **4**, 970–975.

KOROBKIN, A. A. 1996 Asymptotic theory of liquid-solid impact. *Proc. R. Soc. Lond.* A to appear.

LEIGHTON, T. G. 1994 *The Acoustic Bubble.* Academic Press.

PEREGRINE, D. H. 1994 Pressure on breakwaters: a forward look. *Proc. Intl Workshop on Wave Barriers in Deepwaters* pp. 553–573. Port & Harbour Res. Inst. Yokosuka.

PEREGRINE, D. H. & KALLIADASIS, S. 1996 Filling flows, cliff erosion and cleaning flows. *J. Fluid Mech.* **310**, 365–374 (referred to herein as PK).

PEREGRINE, D. H. & TOPLISS, M. E. 1994 The pressure field due to steep water waves incident on a vertical wall. *Proc. 24th Intl Conf. Coastal Engng, Kobe.* ASCE.

RAMKEMA, C. 1978 A model law for wave impacts on coastal structures. *Proc. 16th Conf. Coastal Engng, Hamburg*, vol. 3, pp. 2308–2327. ASCE.

SANGANI, A. S. 1993 A pairwise interaction theory for determining the linear acoustic properties of dilute bubbly liquids. *J. Fluid Mech.* **232**, 221–284.

SCHMIDT, R., OUMERACI, H. & PARTENSCKY, H. W. 1992 Impact loads induced by plunging breakers on vertical structures. *Proc. 23rd Intl Conf. Coastal Engng, Venice*, vol. 2, pp. 1545–1558. ASCE.

SCOTT, J. C. 1975 The preparation of water for surface-clean fluid mechanics *J. Fluid Mech.* **69**, 339–351

TOPLISS, M. E. 1994 Water wave impact on structures. PhD dissertation, University of Bristol.

TOPLISS, M. E., COOKER, M. J. & PEREGRINE, D. H. 1992 Pressure oscillations during wave impact on vertical walls. *Proc. 23rd Intl Conf. Coastal Engng, Venice*, vol. 2, pp. 1639–1650. ASCE.

WALLIS, G. B. 1991 The averaged Bernoulli equation and microscopic equations of motion for the potential flow of a two phase dispersion. *J. Multiphase Flow* **17**, 683–695.

WALSH, J. M., SHREFFLER, M. G. & WILLIG, F. J. 1953 Limiting conditions for jet formation in high velocity collisions. *J. Appl. Phys.* **24**, 349–359.

WATANABE, M. & PROSPERETTI, A. 1994 Shock waves in dilute bubbly liquids. *J. Fluid Mech.* **274**, 349–381.

WIJNGAARDEN L. VAN 1972 One-dimensional flow of liquids containing small gas bubbles. *Ann. Rev. Fluid Mech.* **4**, 369–395.

WIJNGAARDEN L. VAN 1980 Sound and shock waves in bubbly liquids. In *Cavitation and inhomogeneities in underwater acoustics* (ed. W. Lauterborn), pp. 127–140. Springer.

ZHANG, S., YUE, K. P. & TANIZAWA, K. 1996 The impact of a breaking wave on a vertical wall. *J. Fluid. Mech.* To appear.